AD-762 535

BUCKLING OF LONG ROD PENETRATORS

Thomas W. Wright

Ballistic Research Laboratories

Prepared for:

Army Materiel Command

May 1973

BRL MR 2296

BRL

AD

MEMORANDUM REPORT NO. 2296

BUCKLING OF LONG ROD PENETRATORS

by

Thomas W. Wright

May 1973

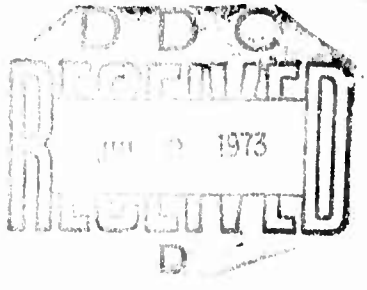

USA BALLISTIC RESEARCH LABORATORIES
ABERDEEN PROVING GROUND, MARYLAND

A11
R

Destroy this report when it is no longer needed.
Do not return it to the originator.

Secondary distribution of this report by originating or sponsoring activity is prohibited.

Additional copies of this report may be obtained from the U.S. Department of Commerce, National Technical Information Service, Springfield, Virginia 22151.

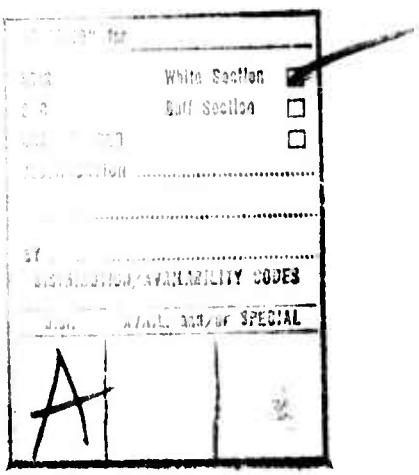

The findings in this report are not to be construed as an official Department of the Army position, unless so designated by other authorized documents.

B A L L I S T I C R E S E A R C H L A B O R A T O R I E S

MEMORANDUM REPORT NO. 2296

MAY 1973

BUCKLING OF LONG ROD PENETRATORS

Thomas W. Wright

Terminal Ballistics Laboratory

RDT&E Project No. 1T061102A33E

A B E R D E E N P R O V I N G G R O U N D, M A R Y L A N D

UNCLASSIFIED
Security Classification

DOCUMENT CONTROL DATA - R & D

(Security classification of title, body of abstract and indexing annotation must be entered when the overall report is classified)

1. ORIGINATING ACTIVITY (Corporate author)	2a. REPORT SECURITY CLASSIFICATION
USA Ballistic Research Laboratory Aberdeen Proving Ground, MD 21005	Unclassified 2b. GROUP

3. REPORT TITLE

BUCKLING OF LONG ROD PENETRATORS

4. DESCRIPTIVE NOTES (Type of report and inclusive dates)

Memorandum

5. AUTHOR(S) (First name, middle initial, last name)

Dr. T. W. Wright

6. REPORT DATE	7a. TOTAL NO. OF PAGES	7b. NO. OF REFS
MAY 1973	37	3

8a. CONTRACT OR GRANT NO.	9a. ORIGINATOR'S REPORT NUMBER(S)
b. PROJECT NO. 1T061102A33E	BRL MEMORANDUM REPORT NO. 2296
c.	9b. OTHER REPORT NO(S) (Any other numbers that may be assigned this report)
d.	

10. DISTRIBUTION STATEMENT

Approved for public release; distribution unlimited.

11. SUPPLEMENTARY NOTES	12. SPONSORING MILITARY ACTIVITY
	U.S. Army Materiel Command 5001 Eisenhower Avenue Alexandria, Virginia 22304

13. ABSTRACT

The dynamic stability of long rod penetrators is examined theoretically. The basic assumption behind the analysis, which is based on a paper by Abrahamson and Goodier, is that plastic bending occurs as a perturbation superimposed on a uniform axial stress. The perturbations are controlled by the strain hardening curve, and the axial stress is the yield stress. The basic analysis introduces nondimensional scaling parameters in a natural way and leads to estimates for time of buckling and the buckled wavelength. The time to buckle is then compared with two load release times, one arising from complete penetration or stoppage and the other from reflections at the rear of the projectile. Tentative design criteria for the dynamic stability of long rod penetrators, based on the time comparisons, are discussed and presented graphically.

DD FORM 1 NOV 68 1473 REPLACES DD FORM 1473, 1 JAN 64, WHICH IS OBSOLETE FOR ARMY USE.

UNCLASSIFIED
Security Classification

14 KEY WORDS	LINK A		LINK B		LINK C	
	ROLE	WT	ROLE	WT	ROLE	WT
penetration mechanics long rod penetrators stability of impact stability diagrams						

BALLISTIC RESEARCH LABORATORIES

MEMORANDUM REPORT NO. 2296

TWright/bst
Aberdeen Proving Ground, Md.
May 1973

BUCKLING OF LONG ROD PENETRATORS

ABSTRACT

The dynamic stability of long rod penetrators is examined theoretically. The basic assumption behind the analysis, which is based on a paper by Abrahamson and Goodier, is that plastic bending occurs as a perturbation superimposed on a uniform axial stress. The perturbations are controlled by the strain hardening curve, and the axial stress is the yield stress. The basic analysis introduces nondimensional scaling parameters in a natural way and leads to estimates for time of buckling and the buckled wavelength. The time to buckle is then compared with two load release times, one arising from complete penetration or stoppage and the other from reflections at the rear of the projectile. Tentative design criteria for the dynamic stability of long rod penetrators, based on the time comparisons, are discussed and presented graphically.

TABLE OF CONTENTS

LIST OF ILLUSTRATIONS

LIST OF SYMBOLS

A	cross sectional area of rod penetrator
c_e	elastic wave speed, $c_e = \sqrt{E_e/\rho}$
c_p	plastic wave speed, $c_p = \sqrt{E_h/\rho}$
d	diameter of solid rod
E_e	elastic bar modulus of rod
E_h	strain hardening bar modulus of rod
$g(\eta,\tau)$	amplification factor of initial velocities
h	target thickness or depth of penetration
k	radius of gyration for cross section of rod
L	length of rod
M	internal moment in rod
P	axial load in rod, $P = \sigma_y A$
p	critical part of g, $p = \tau\eta\|1 - \eta^2\|^{1/2}$
Q	internal shear force in rod
s	nondimensional parameter, $s^2 = \sigma_y/E_h$
t	time
t_p	time for complete penetration or stoppage
t_R	time for reflection from rear of rod
Δu	change in velocity due to elastic impact
v_o	scale factor of initial transverse velocities
v_m	mean velocity of penetration
w	nondimensional transverse deflection, $w = y/k$
w_o	initial nondimensional deflection, $w_o = y_o/k$
x	length along rod from impact end

y	transverse deflection of rod
y_o	initial transverse deflection of rod
$\beta(\eta)$	distribution function for initial velocity
η	nondimensional wave number, $\eta = \pi k/s\lambda$
$\bar{\eta}$	preferred nondimensional wave number
λ	half wavelength of buckles
ξ	nondimensional length, $\xi = sx/k$
ρ	density of rod
σ_y	yield stress of rod in compression
$\Delta\sigma$	change in stress due to elastic impact
τ	nondimensional time, $\tau = s^2 \sqrt{E_h/\rho}\ t/k$
τ_P	nondimensional time of penetration
τ_R	nondimensional time of reflection

I. INTRODUCTION

Recent advances in armor technology have made it desirable to examine the effectiveness of long rod, kinetic energy penetrators. As the length to diameter ratio of the rod increases, the possibility arises that the strong axial forces, imposed on the rod by impact on a target, may give rise to unstable, transverse motions. If the axial load is imposed for a long enough period of time, the transverse displacements may become sufficiently large so that the rod may be said to have buckled. Clearly, severe transverse bending may be expected to degrade the penetration process, particularly in the case of multiple impacts.

It is the purpose of this report to estimate the conditions required to produce transverse instability in long rod penetrators. Penetration mechanics has always been a difficult subject for analysis, and frequently, progress has followed most rapidly from an experimental, rather than an analytical, approach. In this case, however, a simple, linear analysis, published in 1966 by G. R. Abrahamson and J. N. Goodier[1]*, may be used to make explicit estimates of lateral stability. It should be remarked at the outset, however, that the range of validity of the theory has not been completely delineated, since Abrahamson and Goodier reported only a limited set of experiments and obtained only qualitative agreement in some cases.

In the next section, the theory of Abrahamson and Goodier is summarized. In Section III, it is shown how to apply the results of Section II to particular design cases. In Section IV, the direction of future work is indicated.

II. SUMMARY OF THEORY**

When a rod, moving with high axial velocity, strikes a target, large axial stresses may be induced at the impact end. If the rod could respond elastically, a discontinuous increase in stress, given by equation (1), would propagate down the bar with speed c_e .

$$\Delta \sigma = -\rho c_e \Delta u \tag{1}$$

---

*References are listed on Page (21).
**See reference 1 for complete details.

Here, $\Delta\sigma$ is the increase in stress, ρ is the density of material in the rod, c_e is the elastic bar speed ($c_e = \sqrt{E_e/\rho}$, where E_e is the elastic modulus), and Δu is the instantaneous change in velocity of the end of the rod. To see how large $\Delta\sigma$ may be in a representative case, consider a steel rod striking a steel plate with an impact velocity of 4000 fps. In an elastic impact of materials with identical properties, one might estimate Δu to be 2000 fps.* With E_e taken as 30×10^6 psi, and the specific gravity taken as 7.8, the calculated increase in stress comes out to be about 3.5×10^6 psi, which is approximately sixteen times the yield stress of high strength tool steels (e.g., bearcat steel $\sigma_y = 2.2 \times 10^5$ psi).

Clearly, the impact end of the rod cannot sustain such stresses for long, and certainly, such a high stress level cannot propagate into the body of the rod. Instead, the end of the rod is worn away, a stress equal to σ_y, the yield stress, will propagate down the bar with a speed c_e, the elastic bar speed, and stress levels above σ_y will begin to propagate down the bar with a speed dictated by the slope of the strain hardening curve. The speed, c_p, of these additional stresses is often quite small compared to the elastic bar speed;

$$c_p/c_e = 0.13 \text{ to } 0.19$$

in the cases considered by Abrahamson and Goodier. Furthermore, bending that occurs after passage of the elastic wave will depend on the strain hardening modulus, E_h. For the purpose of estimating stability, with the preceding discussion as motivation, the following simplified model is constructed. Refer to Figure 1.

Assume that the stress-strain curve of the bar is bilinear with elastic modulus E_e, yield stress σ_y, and strain hardening modulus E_h (see Figure 2, for example). Since axial loading from longitudinal wave propagation occurs much more rapidly than transverse motion, it is assumed further that the yield stress is applied continuously to the end and in the body of the rod, and that additional bending occurs as a small perturbation so that all longitudinal fibers experience increasing load. Rotatory inertia and shear deformation are neglected, and simple beam theory is applied. The bending moment M is proportional to the second derivative of lateral displacements y.

$$M = -E_h A k^2 \frac{\partial^2 y}{\partial x^2} \qquad (2)$$

*This estimate is based merely on the instantaneous velocity after impact of like materials and has nothing to do with residual velocity.

where A is the cross sectional area of the rod and k is the radius of gyration. Shear force Q induces lateral acceleration.

$$\frac{\partial Q}{\partial x} = \rho A \frac{\partial^2 y}{\partial t^2} \tag{3}$$

Balance of moments requires that

$$Q + P \frac{\partial}{\partial x} (y + y_o) = \frac{\partial M}{\partial x} \tag{4}$$

where P is the axial load, $P = \sigma_y A$, and y_o is the initial deflection.

In the actual boundary valve problems to be examined, the finite rod is assumed to be sufficiently long that, in the analysis, it may be replaced by a semi-infinite rod. Abrahamson and Goodier assumed that both deflection and moment vanish at $x = 0$; $y(0,t) = 0$, $M(0,t) = 0$. These quantities must vanish at infinity as well. Two initial conditions were used: either $y_o(x) = 0$, $\frac{\partial y(x,0)}{\partial t} \neq 0$; or $y_o(x) \neq 0$, $\frac{\partial y(x,0)}{\partial t} = 0$.

Presumably, these two conditions were assumed to give representative results. In any case, the main results turn out to be estimates of times for buckling to occur and characteristic wavelengths in the buckled pattern. The detailed distribution of buckles is not predicted.

The various parameters are expressed in the following nondimensional way.

$$w = \frac{y}{k}, \quad w_o = \frac{y_o}{k} \tag{5}$$

$$\xi = \frac{sx}{k}, \quad \tau = s^2 \sqrt{\frac{E_h}{\rho}} \frac{t}{k} \tag{6}$$

$$s^2 = \frac{\sigma_y}{E_h} \tag{7}$$

Nondimensional displacements are w and w_o, and nondimensional distance and time are ξ and τ respectively. In terms of the variables defined by equations (5) and (6), the equation of motion is

$$w^{iv} + w'' + \ddot{w} = -w_o'' \tag{8}$$

where $w' = \partial w/\partial \xi$ and $\dot{w} = \partial w/\partial \tau$. Since it is assumed that both deflection and moment vanish at $\xi = 0$, the solution may be expressed as a Fourier sine transform

$$w(\xi, \tau) = \int_0^\infty g(\eta, \tau) \sin \eta \xi \, d\eta . \qquad (9)$$

where $g(\eta, \tau)$ must satisfy the ordinary differential equation

$$\ddot{g} - \eta^2 (1 - \eta^2) g = 0 \qquad (10)$$

Initial transverse velocity is supposed to arise[1] "... for instance, from elastic bending waves following a slightly oblique impact", or possibly from previous impacts. If we assume that $w_o(\xi) = 0$ and that initial conditions are given by

$$w(\xi, 0) = 0$$

$$\dot{w}(\xi, 0) = v_o \int_0^\infty \beta(\eta) \sin \eta \xi \, d\eta , \qquad (11)$$

then $g(\xi, \eta)$ is given by

$$g(\xi, \eta) = v_o \beta(\eta) \tau \begin{cases} p^{-1} \sinh p & , \text{ if } \eta < 1 \\ p^{-1} \sin p & , \text{ if } \eta > 1 \end{cases} \qquad (12)$$

where $p = \tau\eta \left|1 - \eta^2\right|^{1/2}$.

Abrahamson and Goodier now argue that large displacements occur when g is large. At each fixed valve of τ, this occurs when p is large and p always has a maximum at $\eta = \bar{\eta} = \frac{1}{\sqrt{2}}$.

The amplification factor of $\beta(\eta)$ in equation (12),

$$\tau p^{-1} \sinh p = \frac{1}{\eta|1 - \eta^2|^{1/2}} \sinh \tau\eta|1 - \eta^2|^{1/2} ,$$

plotted for $0 \leq \eta \leq 1$ with a somewhat arbitrary vertical scale, shows no strong peak at $\tau = 3$, but by $\tau = 6$, a peak is forming, and by $\tau = 9$ the peak is well developed (see Figure 3).

This description does not change much if $w_o(\xi) \neq 0$ with initial conditions taken to be $w(\xi, 0) = \dot{w}(\xi, 0) = 0$. For this case, the preferred value of η is not independent of τ, but decreases with increasing τ. A peak in the amplification factor again forms by $\tau = 6$ and is well developed by $\tau = 9$, but now the peak occurs at a value of η some 12% to 15% larger than before. There is no theoretical reason for singling out the values $\tau = 3$, 6, or 9, but these values do seem to be useful for correlation of the experimental results in reference 1.

The net result is that buckles with nondimensional wave number $\bar{\eta}$ may be expected to have formed by $\tau = 6$ and to be fully developed by $\tau = 9$, provided that loading has been maintained. From equations (5) and (6), this means that buckles of half wavelength λ will form at times t given by

$$\lambda = \frac{\pi k}{s\bar{\eta}} = \pi k \left(2E_h/\sigma_y\right)^{1/2} \tag{13}$$

$$t = \frac{k\tau}{s^2 c_p} = \frac{k\sqrt{E_h \rho}}{\sigma_y} \tau , \tag{13}$$

where τ lies roughly in the range $6 \leq \tau \leq 9$, and buckling will become progressively more severe for still larger times.

III. DESIGN APPLICATIONS

It must be recognized that the conclusions of the last section rest on an incomplete asymptotic analysis. The magnitude and location of buckles cannot be estimated without an explicit statement of initial values and more extensive analysis. For design purposes,

however, the results of the last section may be sufficient if they are interpreted conservatively.

For instability to show up, the loading time must be greater than the time to buckle. There are two unloading mechanisms:

1. The rod penetrates and passes through the target plate, or else it is stopped. In either case, the load is released after time t_p , which may be estimated by

$$t_p = \frac{h}{v_m} \quad .$$

Here h is the target thickness for complete penetration or the depth of penetration otherwise, and v_m is the mean projectile speed during penetration. If uniform deceleration is assumed, v_m is the average of the striking and residual velocities. The nondimensional time to penetrate is

$$\tau_p = \frac{\sigma_y}{E_h} \frac{c_p}{v_m} \frac{h}{k} \quad . \tag{14}$$

Comparison of τ_p with any other time τ shows that the ratio

$$\tau_p/\tau \quad \text{is } >, =, \text{ or } < 1$$

according as

$$\frac{v_m}{c_p} \text{ is } <, = , \text{ or } > \frac{1}{\tau} \frac{\sigma_y}{E_h} \frac{h}{k} \tag{15}$$

2. The elastic wave reflects from the rear end of the rod where the stress drops back to zero. The unloading wave then propagates at the elastic bar speed back to the impact end. The time required for the round trip is

$$t_R = \frac{2L}{c_e} = \frac{2L}{\sqrt{E_e/\rho}}$$

The nondimensional time is

$$\tau_R = \frac{2\sigma_y}{\sqrt{E_h E_e}} \frac{L}{k} \quad . \tag{16}$$

Comparison of τ_R with any other time τ shows that the ratio

$$\tau_R/\tau \text{ is } >, =, \text{ or } < 1$$

according as

$$\frac{L}{k} \text{ is } > , = , \text{ or } < \frac{\tau}{2} \frac{\sqrt{E_h E_e}}{\sigma_y} \tag{17}$$

If loading is maintained at the impact end, the loading wave will be reinitiated. It seems likely that the resultant cyclic loading and unloading for a given length of time will be less likely to cause buckling than sustained loading for the same length of time. Furthermore, if buckles do form, they will probably be less severe. These facts should be accounted for in establishing design rules.

Equations (15) and (17) are the primary results with design implications in this memorandum. For τ = 3, 6, and 9, these two equations are plotted in Figures 4 and 5. Radius of gryation k has been replaced by the symbol d/4. For a solid rod of uniform material throughout, d is the diameter.

Figures 4 and 5 are to be used as follows. For a given long rod penetrator and a given target, the numbers l, d (or k), E_h, E_e, σ_y, and ρ are known. E_h, E_e, and σ_y should be obtained, preferably, from carefully run compression tests. Then $c_p = \sqrt{E_h/\rho}$ may be computed, and for a given impact velocity, the numbers v_m and h must be estimated. Next, the ordinates and abscissas for the two figures may be computed and a point located in each figure. The range of values of τ_p or τ_R that corresponds to each wedge shaped region has been indicated on the figures. Examination of the experimental results of Abrahamson and Goodier show that tentative interpretation of the points, so located in the various wedges of Figures 4 and 5, might be as follows. In each case, τ_p is considered

first, and interpretation is then conditioned by τ_R . The design rule is stated first in italics, followed by a few explanatory comments.

i) *If* $\tau_P < 3$, *then the rod is probably safe for any* τ_R . In other words, the time of penetration is sufficiently short that the impact end unloads before buckles have time to develop no matter how long the rod.

ii) *If* $3 < \tau_P < 6$, *then the rod is probably safe if* $\tau_R < 9$, *but it may be only marginally safe if* $\tau_R > 9$. The load is now maintained at the impact end for a long enough time that buckling may be incipient unless unloading by reflection from the free end also occurs. If buckles do begin to form, the amplitudes (maximum deflection from the straight rod) will be small. In subsequent impacts, the incipient buckles will tend to be amplified.

iii) *If* $6 < \tau_P < 9$, *then the rod is probably safe if* $\tau_R < 6$, *and marginally safe for* $6 < \tau_R < 9$. *If* $\tau_R > 9$, *the rod may still be marginally safe.* The same comments as for ii) apply here as well, but now since time of penetration is more severe, the time for reflection judged to be safe has been reduced.

iv) *If* $\tau_P > 9$, *then the rod may be safe for* $\tau_R < 3$, *but for* $3 < \tau_R < 6$, *it is only marginally safe. For* $6 < \tau_R < 9$ *the rod may still be marginally safe provided* $\tau_P < 2\ \tau_R$, *but if* $\tau_P > 2\ \tau_R$ *or if* $\tau_R > 9$, *then buckles will probably form.* The longer the loading time τ_P or the larger the ratio τ_P/τ_R , the more severe the buckling will be. In this case, the load is maintained at the impact end for a sufficiently long time to develop buckling. For short rods, however, the load is periodically released from the rear end so that the transverse motion must be reinitiated each time the axial loading passes by. As τ_P and τ_R increase, there is enough time for buckles to develop either during one passage of the axial wave ($\tau_P > 9$, $\tau_R > 9$) or during multiple passages of the axial wave ($\tau_P > 9$, $6 < \tau_R < 9$, but $\tau_P/\tau_R > 2$ or 3). There is nothing in the analysis that indicates the conditional effect of τ_R for large τ_P (i.e. $\tau_P > 9$) as stated here. Rather, it is inferred from examination of the experimental results of Abrahamson and Goodier, and it is consistent with those results.

The interpretation of the last four paragraphs is only tentative because the analysis of Abrahamson and Goodier does not predict the severity of buckling. Furthermore, their experiments were not designed

to find criteria for the marginal onset of buckling, but rather were intended to demonstrate the wavelength relationship once buckling had definitely occurred. Finally, their rods were made from 6061 - T6 and 2024 - T3 aluminum, rather than high strength steels or high density materials, and it has not been demonstrated that the theory will then apply. Therefore, the above conclusions cannot be drawn directly from the data, but represent an extrapolation of some sort.

Still further extrapolation is required to apply these results to technologically important cases. Figure 2 shows an idealized stress-strain curve for bearcat steel. The ratio

$$c_p/c_e = \sqrt{E_h/E_e} = 0.152 \quad ,$$

computed from the curve, falls in the same range as in the experiments of Abrahamson and Goodier (0.13 to 0.19) so that the rate of plastic loading compared to elastic loading is similar. On the other hand, the important ratio $\sigma_y/E_h = 0.319$ for bearcat, but only 0.13 to 0.25 for aluminum in reference 1, so that the stress strain curves are only approximately similar. Furthermore, impact conditions may vary widely from those used in reference 1. As noted in the introduction, the ratio $\Delta\sigma/\sigma_y \simeq 16$ for an impact velocity of 4000 fps in bearcat, but the maximum in all the experiments of Abrahamson and Goodier is $\Delta\sigma/\sigma_y \simeq 8$, so that the excess energy available above the elastic strain energy absorbed at yield is greater for typical impacts with bearcat rods. In addition, the ratio v_m/c_p for bearcat ($c_p \simeq 2560$ fps) may well be in the range of 1.5 or 2.0, whereas the maximum in reference 1 is only 0.29. Finally, in the experiments there were no significant penetrations, and the impact ends of the rods, although slightly mushroomed in some cases, were never actually worn away.

In spite of these reservations, figures 4 and 5, if used conservatively, should be helpful at least for preliminary design. In figure 4, the vertical and horizontal lines have been drawn for bearcat steel with ratios of h/d = 1, 2, 5, 10, and 15 and mean penetration velocities of v_m = 2000, 4000, and 6000 ft./sec. In figure 5, vertical lines corresponding to bearcat steel, 6061-T6 aluminum, and 2024-T4 aluminum are shown. Other materials could be plotted as well of course.

IV. FUTURE WORK

At the end of the last section, it was indicated that, in many respects, applications may well fall outside the limits of experimental verification. Further experimentation can readily show whether or not

the scaling is shown to be valid, however, there remains the fact that it applies only to the case of normal incidence without yaw. These two factors, oblique incidence and yaw, will certainly introduce transverse forces on the impact end of the rod and may introduce a transient moment as well. Axial compression will tend to amplify the bending in these cases. An investigation of the effect of transverse end forces or end moments on solutions of equation (8) is currently underway and will be reported upon in the near future.

REFERENCE

1. G. R. Abrahamson and J. N. Goodier, Dynamic Flexural Buckling of Rods Within an Axial Compression Wave, J. Appl. Mech., 33, 241 - 247 (1966).

APPENDIX

BUCKLING OF LONG ROD PENETRATORS

T. W. Wright
Aberdeen Proving Ground, Md.
November 1972

Figures 1 - 5

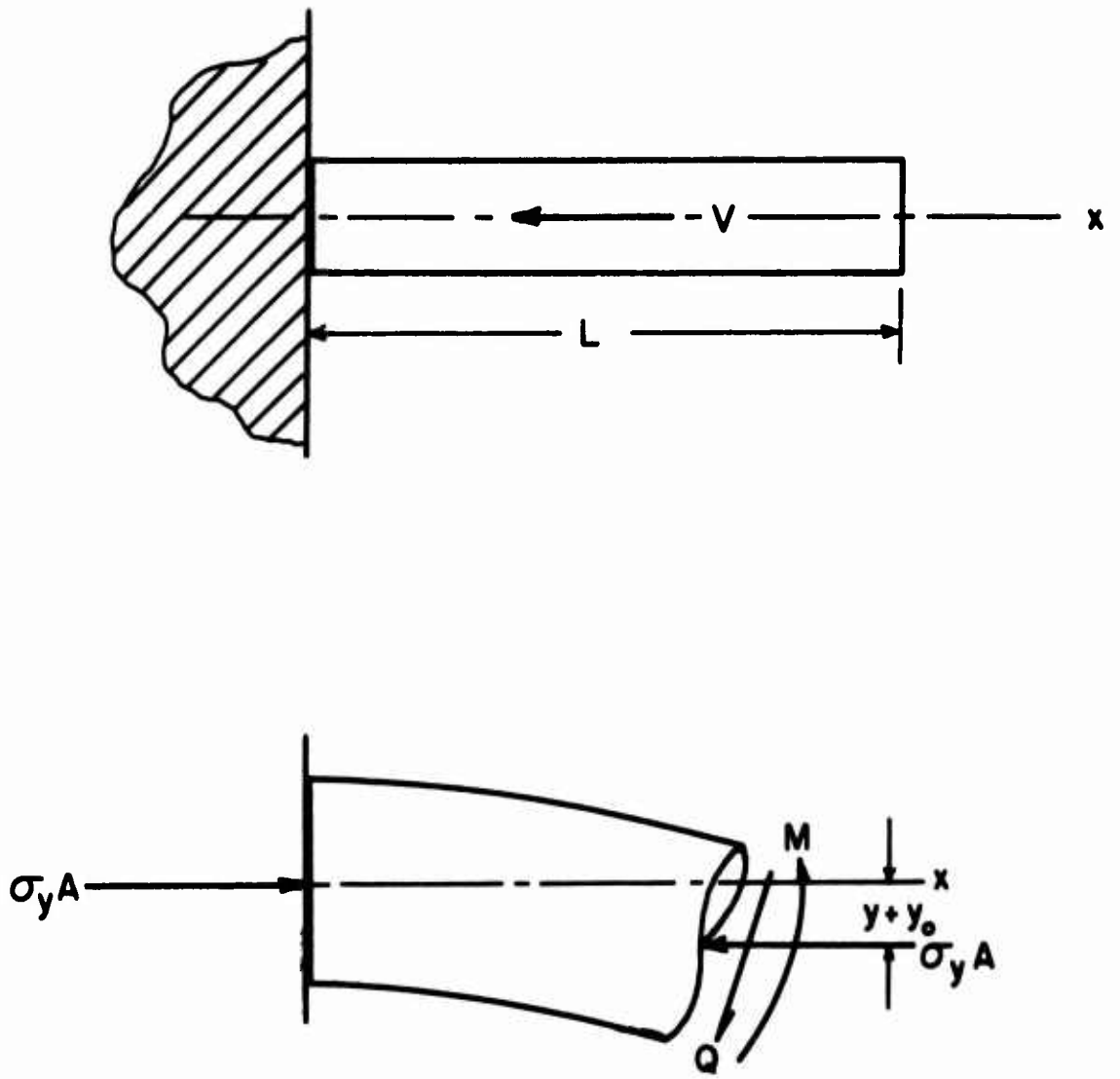

Figure 1. Impact Geometry and the Assumed Internal Loads.

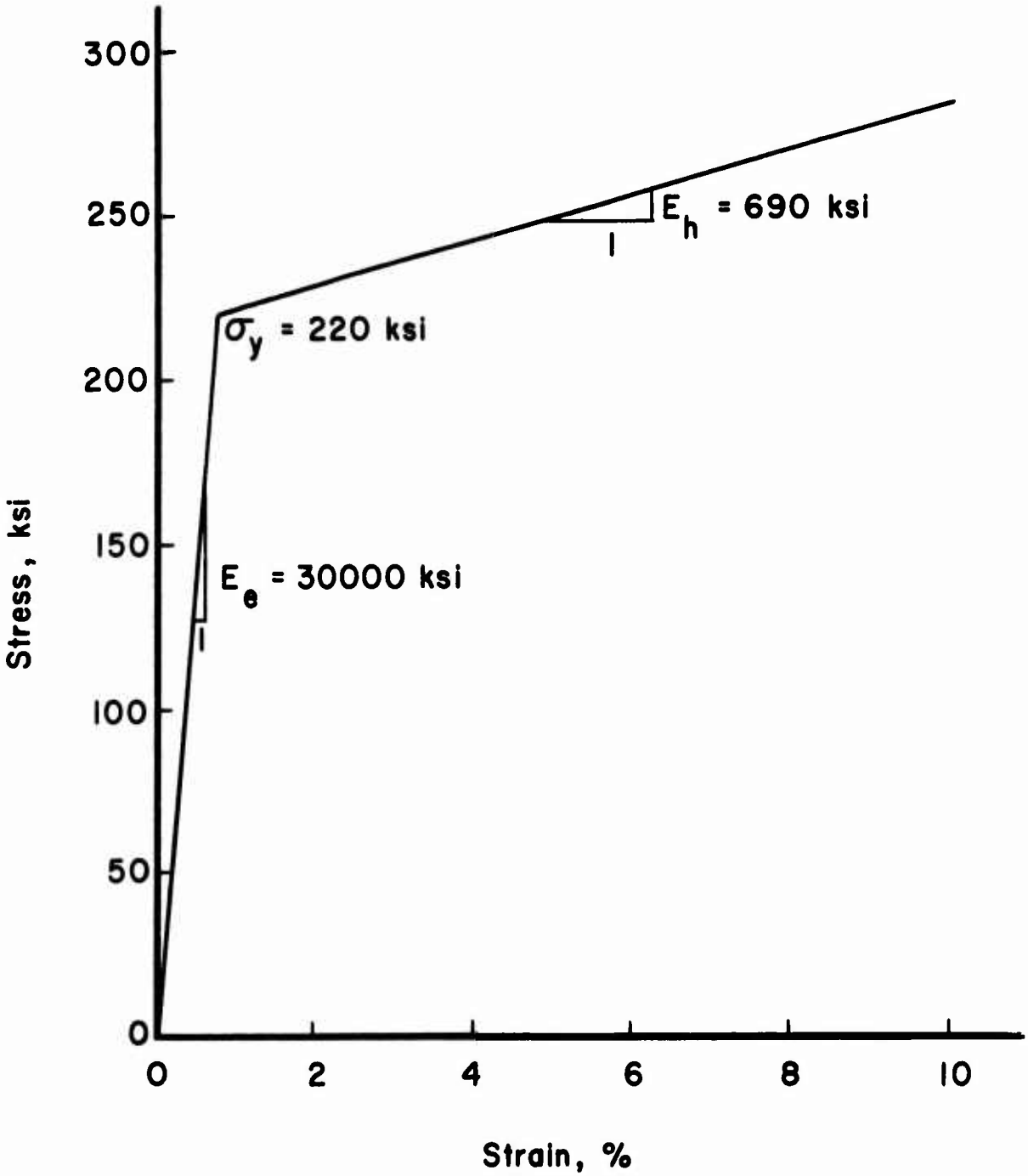

Figure 2. Idealized Stress-Strain Curve for Bearcat Steel.

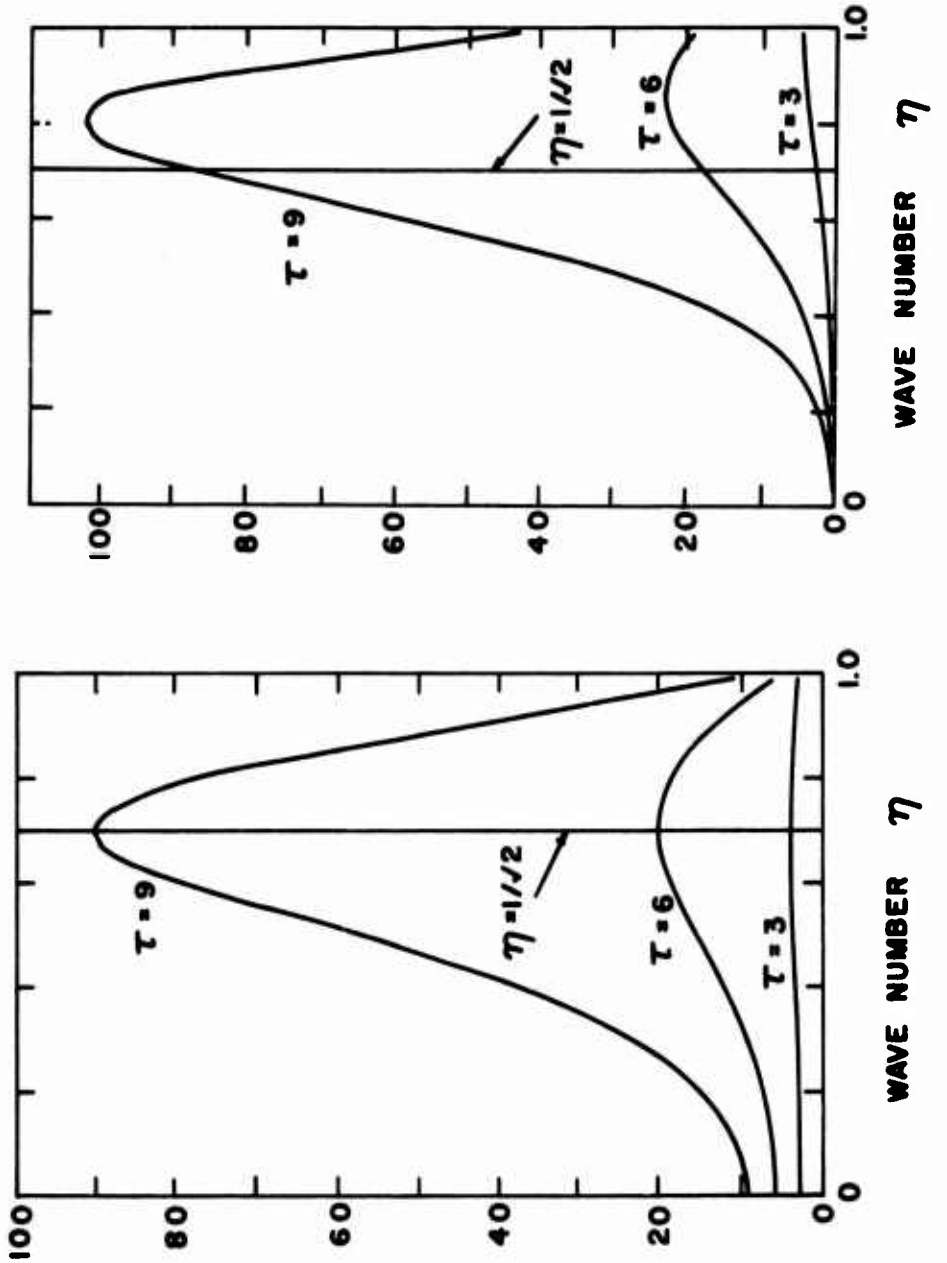

Figure 3. Amplification Factors (after Abrahamson and Goodier).

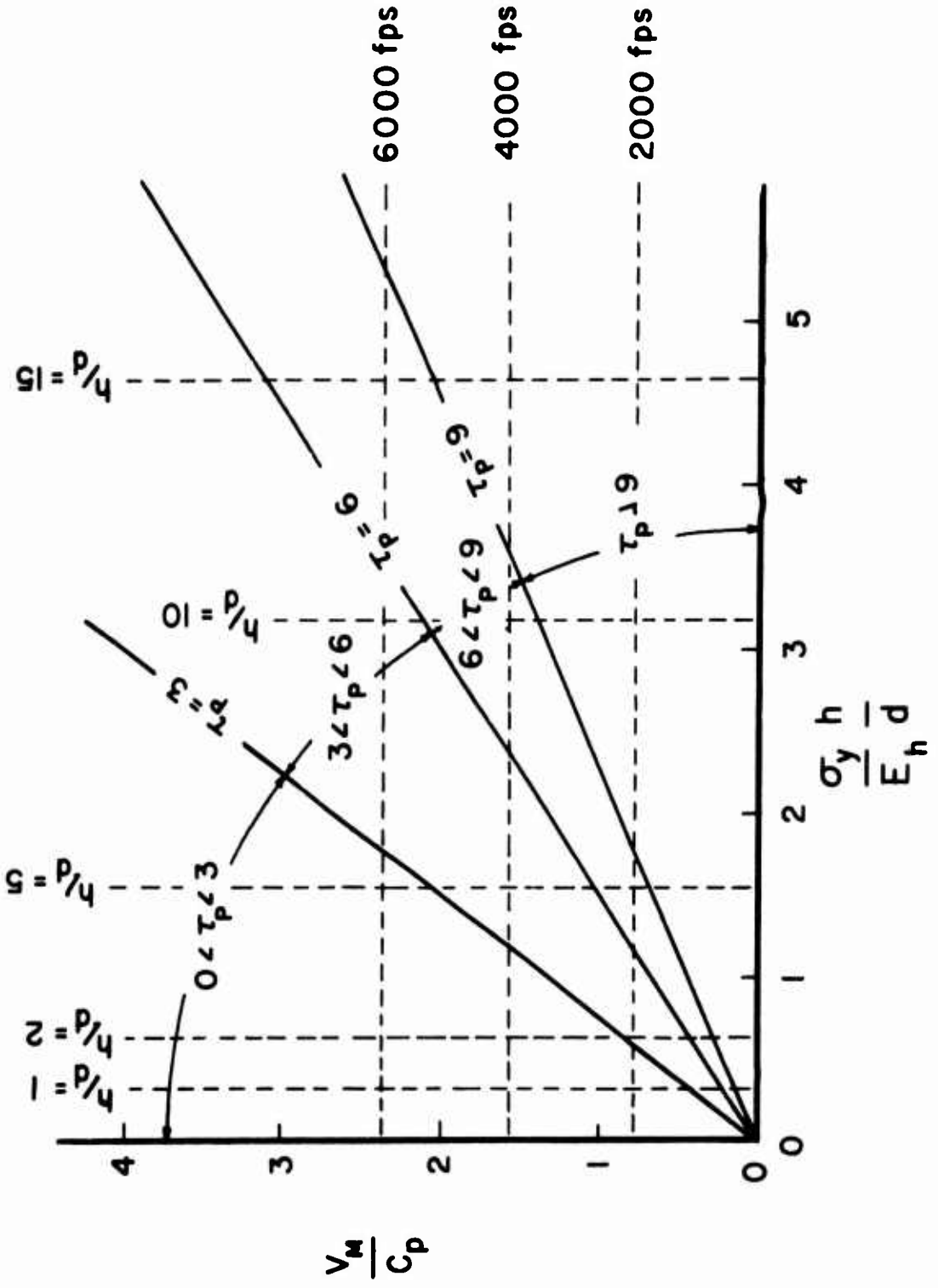

Figure 4. Time of Load Release from Complete Penetration or Stoppage.

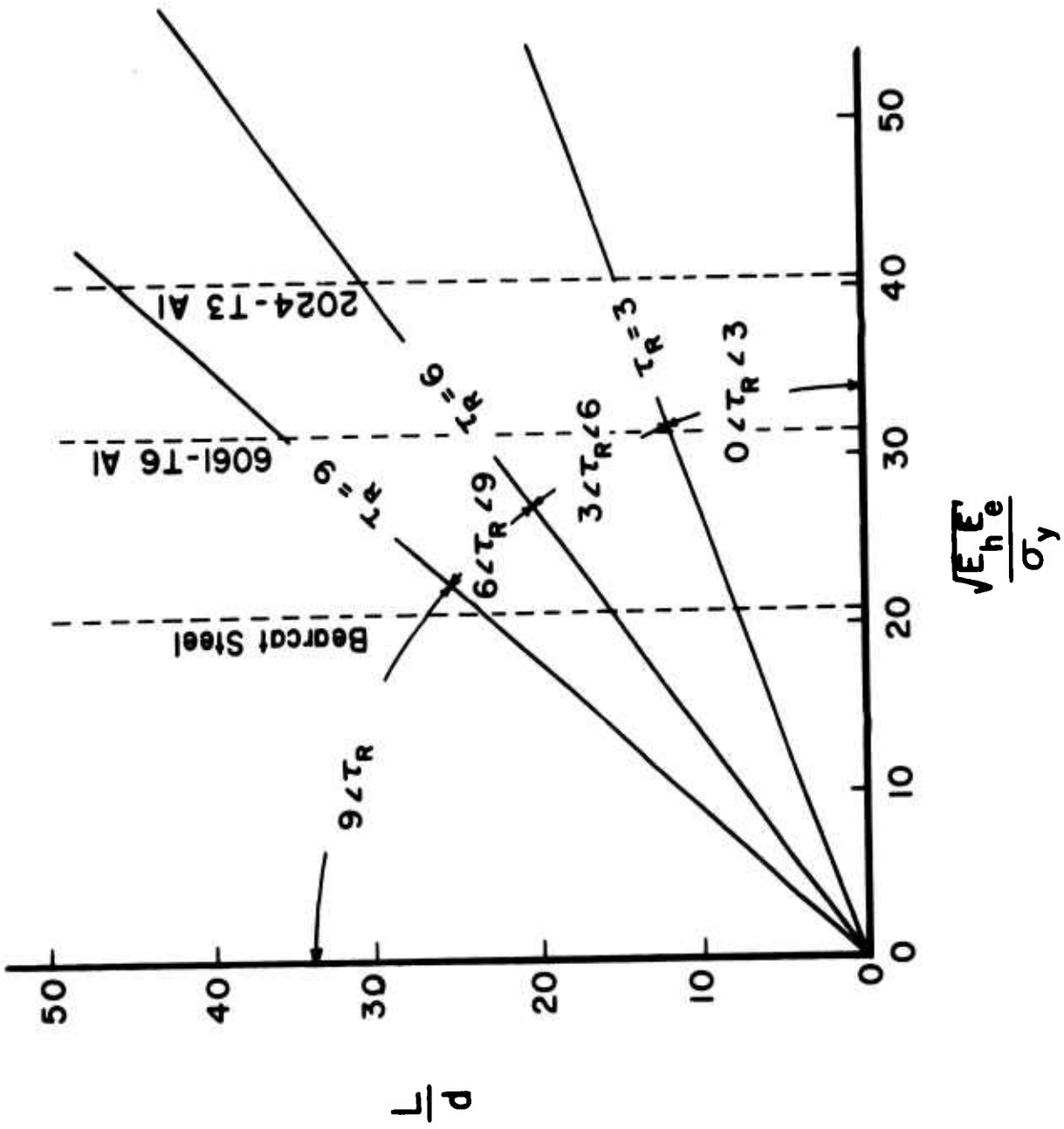

Figure 5. Time of Load Release from Reflections at Rear of Projectile.